

DRAFT

GTINDIA2019-2442

SAVONIUS WIND TURBINE BLADE PROFILE OPTIMIZATION BY COUPLING CFD SIMULATIONS WITH SIMPLEX SEARCH TECHNIQUE

Ankit Agrawal

M. Tech. Student

Department of Mechanical Engineering
Indian Institute of Technology Guwahati
Guwahati – 781039, Assam, India.

Deepak Sharma

Associate Professor

Department of Mechanical Engineering
Indian Institute of Technology Guwahati
Guwahati – 781039, Assam, India.

Divyeshkumar D. Kansagara

M. Tech. Student

Department of Mechanical Engineering
Indian Institute of Technology Guwahati
Guwahati – 781039, Assam, India.

Ujjwal K. Saha*

Professor

Department of Mechanical Engineering
Indian Institute of Technology Guwahati
Guwahati – 781039, Assam, India.

ABSTRACT

The Savonius rotor, a drag-based vertical axis wind turbine, is characterized by its design simplicity, low noise level, self-starting ability at low wind speed and low cost. However, its low performance is always a major issue. One of the remedies of this issue is to design an optimized rotor blade profile, which has mostly been developed through trial and error approach in the literature. In this paper, an optimum blade profile is obtained by maximizing its power coefficient (C_P) by coupling CFD simulations of rotor blade profile with the simplex search technique. Since the blade profile is symmetric about its axis, half of the blade geometry is created through natural cubic spline curve using three points. Two of them are kept fixed, whereas the other one is changed through optimization technique in its every iteration using MATLAB platform. In every iteration, the blade profile is meshed using ANSYS ICEM CFD. The analysis of the blade profile is performed through ANSYS Fluent by using shear-stress transport $k-\omega$ turbulence model. A finite volume method based solver is used to solve the transient 2D flow around the wind turbine. The optimum profile of the blade is compared with the conventional profile over a wide range of tip speed ratios (TSRs) in order to check its feasibility for practical applications. The optimum blade profile is found to be better than the semicircular blade in the range of $TSR=0.6-1$.

Keywords: Savonius rotor; blade profiles; power coefficient; tip-speed ratio; CFD simulations; Simplex search technique

*Corresponding author

Email: saha@iitg.ernet.in

Tel: 0091-361-2582663; Fax: 0091-361-2690762

NOMENCLATURE

CFD	Computational Fluid Dynamics	--
C_P	Power coefficient	--
C_T	Torque coefficient	--
DCT	Discrete Cosine Transformation	--
D	Overall diameter of blade profile	[m]
F_L	Lift force	[N]
F_D	Drag force	[N]
L	Chord length of blade profile	[m]
$HAWT$	Horizontal Axis Wind Turbine	--
N	Rotational speed of rotor	[rpm]
OR	Overlap Ratio	--
r	radius of blade profile	[m]
$RANS$	Reynolds-Averaged Navier-Stokes	--
RPM	Revolution per minute	--
SG	Separation gap	--
SST	Shear Stress Transport	--
t	Thickness of the blade	--
TSR	Tip Speed Ratio	--
U_o	Free stream wind speed	[m/s]
V_i	Tangential velocity of the blade profile	[m/s]
$VAWT$	Vertical Axis Wind Turbine	--

Greek Letters

β	Constant	--
γ	Constant	--
θ	Sectional cut angle	[°]
k	Turbulent kinetic energy	[m ² /s ²]
ε	Turbulence dissipation rate	[m ² /s ³]
ω	Specific turbulence dissipation rate	[s ⁻¹]
ω_z	Rotor rotational speed	[rad/s]

1 INTRODUCTION

Energy is an indispensable requirement for human growth and development. Much of it is derived from burning fossil fuels such as coal, gas and oil. These sources are termed as non-renewable energy sources and have only a limited presence in the nature. As per the CIA fact book, if the present rate of consumption continues, all the resources of these fossil fuels will be completely consumed by the year 2100. Another demerit of using them is the pollution, which ultimately leads to health hazards and global warming. Therefore, an urgent shift needs to be made towards using more of renewable energy sources such as the wind energy. It is mostly harvested in open environments such as offshores using horizontal axis wind turbines (*HAWT*). However, wind energy can also be generated in the dense urban areas using vertical axis wind turbines (*VAWT*). One such *VAWT* is the Savonius wind turbine. It has several qualities such as compactness, simple assembly, omnidirectionality, self-starting ability at low speed, low cost etc. Still, the performance of the conventional Savonius wind turbine having semicircular blades is relatively low and numerous attempts have been made to improve it.

Fernando and Modi [1] used wind tunnel tests to assess the effects of different system parameters on the performance of Savonius wind turbine. Fujisawa [2] studied the performance and the flow fields of Savonius rotors at various overlap ratios (*ORs*) and suggested that the maximum power coefficient (C_{Pmax}) is found on the *OR* of 0.15 and it decreases as the *OR* is further increased. Gupta and Sharma [3] also showed that maximum C_P of 0.25 was obtained at 20% overlap condition. Similarly, power and torque coefficients (C_P and C_T) decrease with the increase of overlap from 0% to 16.2%. Saha et al. [4] conducted wind tunnel tests and found the optimum number of blades to be two for any staged Savonius turbine. They also found a higher C_P for a twisted-bladed turbine as compared to a semicircular bladed turbine. It was also shown that the two staged Savonius turbine had a better C_P as compared to single- or three-staged Savonius turbines. Mahmoud [5] also found the two-bladed rotor to be more efficient than three- and four-bladed rotors. The rotor with end plates gives higher efficiency than those without end plates. Jeon et al. [6] experimentally studied the effects of end plates with various shapes and sizes on the performance of helical-bladed Savonius wind turbines with twist angles of 180° and two semicircular-bladed turbines and observed the C_P to increase linearly in proportion to the area of the end plate. The use of both upper and lower circular end plates significantly increased the C_P by 36% compared to the one without end plates.

Akwa et al. [7] did computational analysis and their results were found to be in agreement with experimental data [2, 3]. The maximum turbine performance for blade *OR* ≈ 0.15 gives an averaged C_P equal to 0.316 for the *TSR*=1.25. Roy and Saha [8] carried out unsteady two-dimensional study to observe the effect of *ORs* on static torque characteristics and found the effects of negative static torque coefficient to be eliminated at

OR=0.20, and it provides a low static torque variation at different turbine angular positions giving a higher mean static torque coefficient as compared to the other *ORs*. Alom et al. [9] tested the elliptical-bladed profiles at different sectional cut angles of $\theta = 45^\circ, 47.5^\circ, 50^\circ$ and 55° and found that the elliptical profile with $\theta = 47.5^\circ$ showed a C_{Pmax} of 0.33 at *TSR* = 0.8, whereas the conventional semicircular profile indicated a highest C_{Pmax} of 0.27. Roy et al. [10] used differential evolutionary algorithm, an inverse optimization method and reduced the overall area by up to 9.8% of the Savonius turbine for a given torque and power. Chan et al. [11] incorporated CFD simulations into the genetic algorithm to numerically optimize the conventional semi-circular blade profile of the savonius wind turbine. Zhou et al. [12] investigated the geometry optimization ability of evolutionary algorithms based on two-dimensional discrete cosine transformation (2D-DCT) through numerical simulations and improved the efficiency by 13.77% at *TSR*= 1.0.

From the literature, it can be observed that initial studies focused on designing the blade profile by trial and error method. Later advanced optimization techniques such as evolutionary algorithms are used, which are always computationally expensive. In this paper, a numerical direct search technique is used, which is coupled with *CFD* simulations in order to develop a complete automated procedure for blade shape optimization of the conventional Savonius wind turbine.

2 OPTIMIZATION ALGORITHM

In this paper, the simplex search method [13] is used for optimization, which is one of the most popular direct search numerical optimization techniques in the literature. The method starts by creating a non-zero volume hypercube/simplex using $(N + 1)$ points in an N -dimensional variable space. The objective function is then calculated at those points. Based on their objective function values, these points are categorized into the worst point (x_h), best point (x_b), and next to the worst point (x_g). For maximization problem, x_h is referred to a point which has the lowest objective function value. Similarly, x_b shows the maximum function value among rest of the N points. Since this method is developed to move away from the worst point, the centroid (x_c) of all but the worst point is calculated and x_h is reflected through x_c as $x_r = 2x_c - x_h$. The objective function is then calculated at the reflected point, x_r . If the objective function value of x_r is better than x_b , then the new point is further expanded as $x = (1 + \gamma)x_c - \gamma x_h$, where γ is constant and its value is greater than one. In case x_r is worse than x_h , the new point is contracted as $x = (1 - \beta)x_c + \beta x_h$. Here, β is another constant and its value lies between 0 and 1. If x_r is better than x_h , but worse than x_g , then the new is contracted as $x = (1 + \beta)x_c - \beta x_h$. The new point created by any of the above cases is then included into the simplex by removing x_h . The procedure continues till a maximum number of iterations is

reached or a difference between the new point and the best point is less than some smaller value (ϵ).

2.1 Savonius Turbine Geometry

A conventional savonius wind turbine with two identical semi-circular blades is presented in Figure 1 along with other parameters. The chord length (L) of one semi-circular blade is 100 mm with a uniform thickness (t) of 2 mm. The blades rotate periodically around the centre O ($0,0$) with a diameter D ($=2r$) with an angular velocity ω_z . The two blades are separated by a spacing (SG) and an overlap (OR).

The x coordinate is set along the incoming wind which is set at a speed of $U_o = 7.30$ m/s [11]. The y coordinate is along the cross-stream direction. Since the aim of the current work is to optimize the blade shape, the separation gap, SG and overlap ratio, OR are neglected, i.e, $SG = OR = 0$. The TSR is set at a constant value of 0.8 and the corresponding angular velocity is $\omega_z = 58.4$ rad/s.

2.2 Optimization Problem Formulation

The formulation of shape optimization of the blade profile of conventional Savonius wind turbine [11] shown in Figure 1 is given as

$$\begin{aligned} & \text{Maximize } C_T(x,y) \\ & \text{subject to } 0 < x < L, 0 < y < 0.75L \end{aligned} \quad (1)$$

Here, C_T is the time averaged torque coefficient, and x and y are the coordinates of a point. Since two ends of the half of the blade are fixed, only one intermediate point is used to design the profile using natural cubic spline curve. The coordinates x and y of the intermediate point thus become the design variable of the given optimization problem. As mentioned earlier, C_T is calculated using ANSYS ICEM CFD and ANSYS Fluent, only direct search method can be used for optimizing the given problem. It is to be noted that a bracket operator-based penalty function method is used.

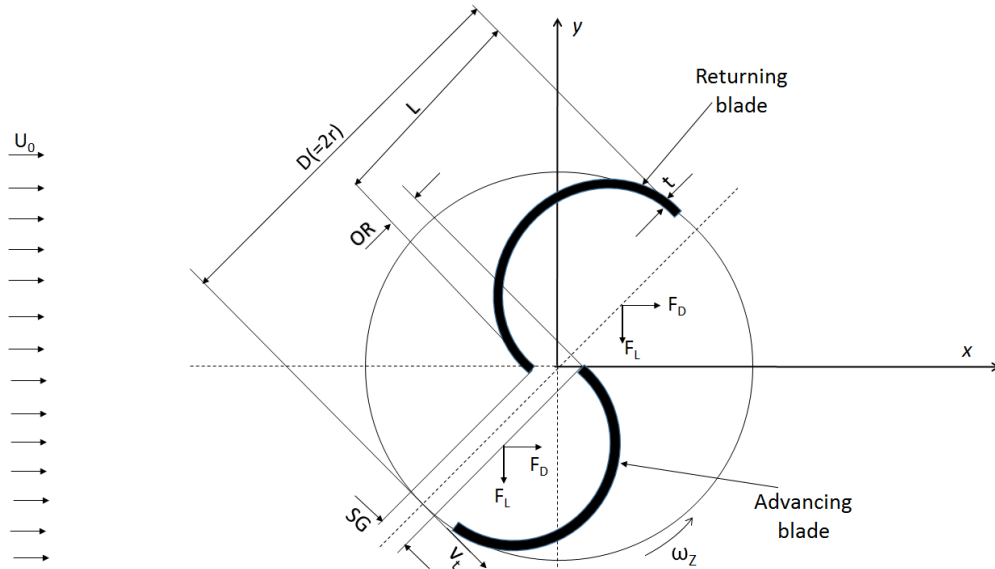


Figure 1: A typical two semicircular-bladed Savonius wind turbine

2.3 Methodology

As shown in Figure 2, an automated process is deployed for the blade shape optimization which couples the blade geometry definition, mesh generation and objective function evaluation with CFD simulations. MATLAB is employed as the workflow platform, calling all codes sequentially. Since the number of decision variable is two, as per simplex search method three random initial points need to be provided that lie within the search space. Each of these points is used with two other fixed points which are $(0,0)$ and $(L,0)$ to define one blade profile as shown in Figure 3. Now, a natural cubic spline is fit using these two fixed points and one variable point. This gives a blade skeleton which is then given an offset of value ' t ' to

obtain the inner and outer surface points of the blade. All the points which lie on the surface of the blade are extracted and saved into a .txt file in a particular format. Similarly, the other two variable points chosen initially are used to provide two more blade geometries. Once the formatted data points are stored in the text file for the different blade geometries, ANSYS ICEM CFD is launched. This software package is used to import all these data points to form the respective geometries. Once the geometry is imported, it can be meshed and then the meshed file is stored in a format which is acceptable by ANSYS Fluent for carrying out further simulations. The whole process can be recorded and saved into

a script file for automating the whole geometry and meshing process. Now ANSYS Fluent is launched and the solution setup is given and simulations are carried out. The results are again saved into text file. All the operations in ANSYS Fluent are also recorded in a journal file in order to automate the process for future iterations. The text file carrying the results of the simulation is read by the MATLAB code and the time averaged C_T obtained is the objective function value for the given

problem. Then, the algorithm of simplex search method combined with bracket operator penalty method is executed to generate new points. This process is carried out until the termination conditions are met. Once the final optimum blade shape is obtained, it is compared with the conventional semicircular rotor blade profile over a wide range of TSR .

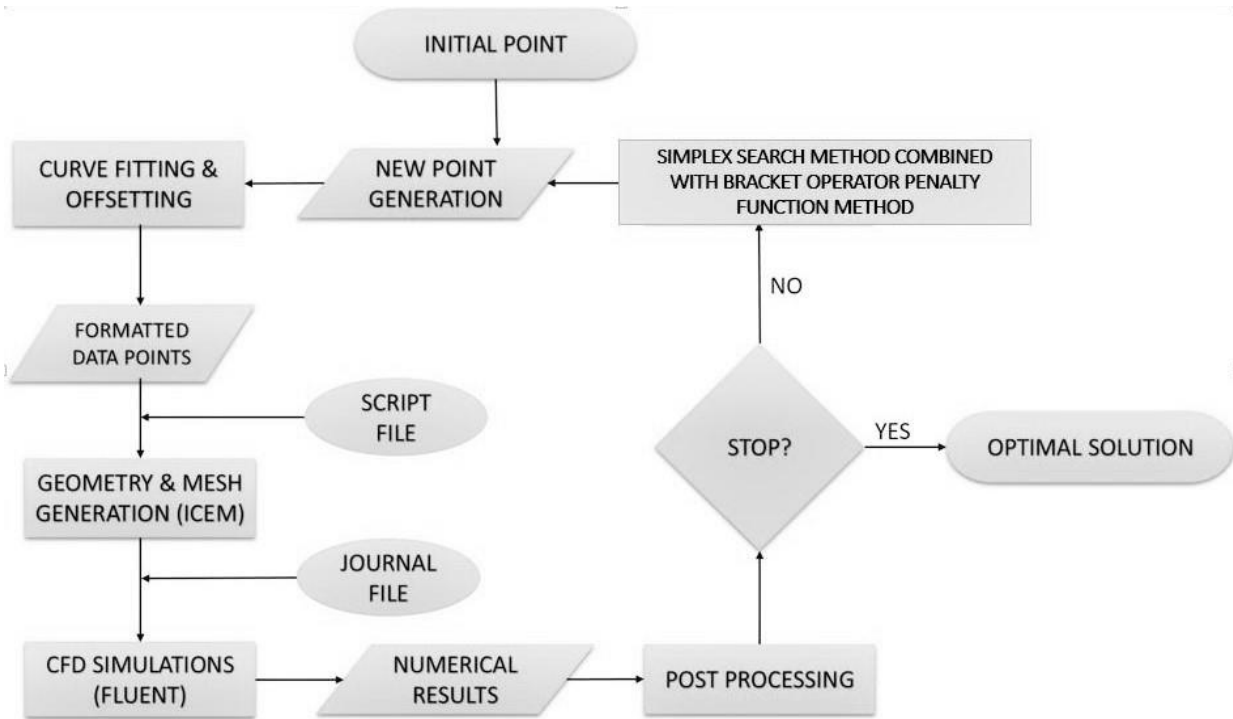


Figure 2: Process flowchart

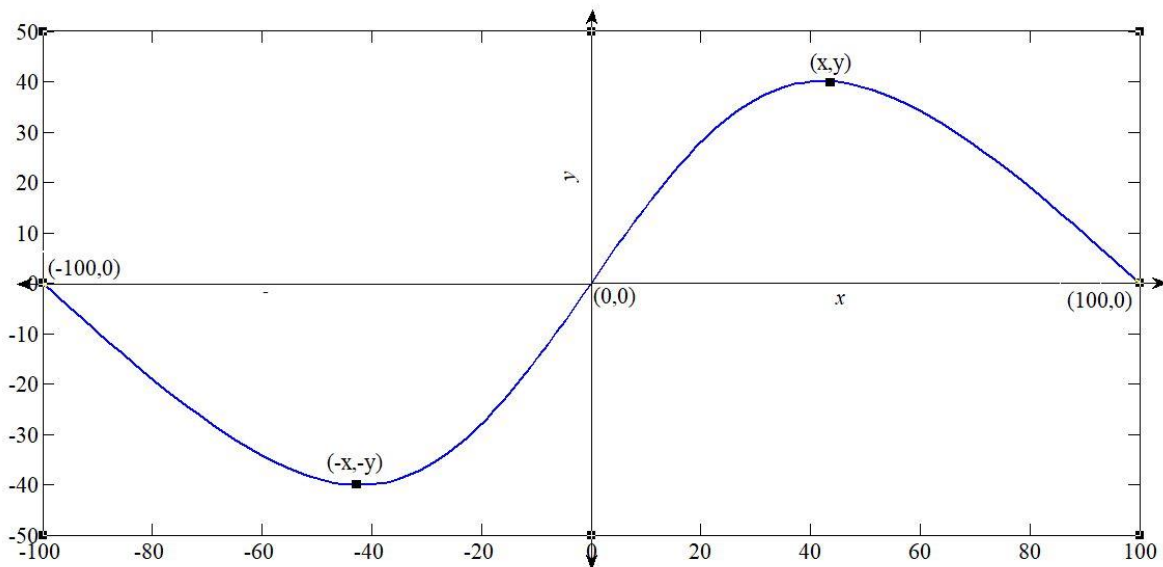


Figure 3: Blade skeleton with fixed and variable points

3 NUMERICAL SIMULATION ASPECTS

This section includes computational domain and its boundary conditions, the meshing of the domain, grid independency test, implementation of the turbulence model, and the solver set-up. These are explained below.

3.1 Computational Domain and Boundary Condition

The computational domain is illustrated in Figure 4. It can be categorised into two parts, i.e., a rotational zone around the turbine blades and a non-rotational outer zone. The rotational zone houses the turbine blades and their centres coincide at the origin. The diameter of the turbine blade is D and that of the rotational zone is $2D$. The non-rotational outer zone is a rectangle. The upper and lower horizontal edges are located at a distance of $7.5D$ from the origin and are given part name ‘Symmetry’. The left vertical edge, named ‘Inlet’ is located at a distance of $7.5D$ before the origin, while the right vertical edge, named ‘Outlet’ is located at a distance of $15D$ from the origin. The inlet is given a boundary condition of velocity inlet with an incoming velocity of 7.30 m/s [11] and a turbulent intensity of 1% . The ‘Pressure outlet’ condition is used for outlet with same value of turbulent intensity. The upper and lower edges are given ‘Symmetry’ boundary condition. The blade surface is set to ‘wall’ and further moving wall, rotational motion and no slip conditions are selected. There is an interface named ‘Int’ between the two zones. The size of the outer zone is chosen such that there is no effect of the boundaries on the turbine performance.

3.2 Meshing

Unstructured mesh with all tri elements is used throughout the domain. The sliding mesh option is used at the interface between the rotational and the non-rotational zone and is given a rotational speed of 58.4 rad/s corresponding to the TSR value of 0.8 . Figure 5 shows the mesh images of non-rotational zone while Figure 6 shows the mesh images of rotational zone and Figure 7 shows the mesh images of both these parts combined.

3.3 Turbulence Model

A finite volume method based solver, ANSYS Fluent is used to solve unsteady Reynolds-Averaged Navier Stokes (RANS) equation to conduct two dimensional transient simulations. The turbulent viscosity terms in the RANS equation is calculated using the shear-stress transport (SST) $k-\omega$ turbulence model. The SST $k-\omega$ turbulence model combines the advantages of both $k-\epsilon$ model for free stream flows and the $k-\omega$ model for boundary layer flows to ensure that the flow separation with adverse pressure gradients is predicted accurately.

3.4 Solver Setup

The second order upwind scheme is used for the spatial discretization of momentum, turbulent kinetic energy and specific dissipation rate. The second order scheme is used for pressure while the least squares cell based scheme is used for gradient. The *SIMPLE* scheme is used for pressure velocity coupling.

3.5 Grid Independence Test

A blade profile generated using one of the optimum points from Chan et al. [11], i.e., (60.84,35.65) is used to carry out the grid independency test. Three sets of mesh were tested and the results are mentioned in table 1. The total number of elements in the three meshes varies from 65000 (Mesh 1) to 100000 (Mesh 2) and then to 140000 (Mesh 3). The time averaged C_T values at a constant time step of 2.988755×10^{-4} s for the three meshes are 0.2309, 0.2357 and 0.2363 and the corresponding time (in hours) required to complete the simulations was 4.25, 6 and 8.5. It can be seen that C_T increases by 2.07% from mesh 1 to mesh 2 and the increase in the time taken is not more than 2 hours. From mesh 2 to mesh 3, C_T increases by 0.25% while the time taken to complete the simulation increases by 2.5 hours. Therefore, in order to save the computational effort, mesh 2 is selected for the present study.

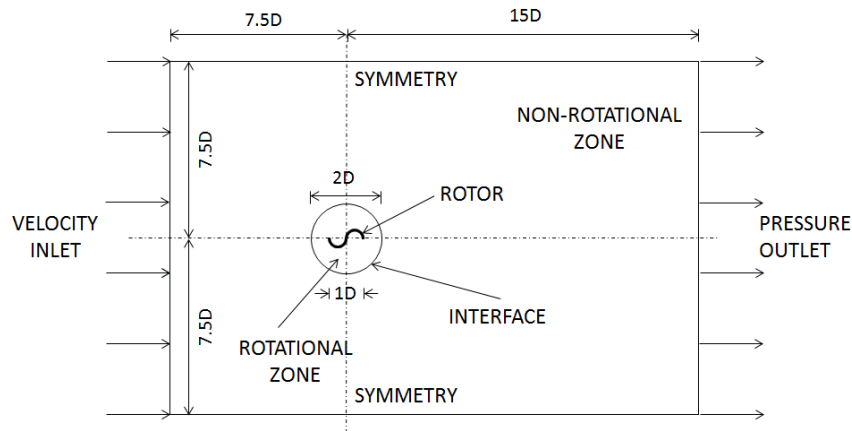


Figure 4: Computational domain and boundary conditions

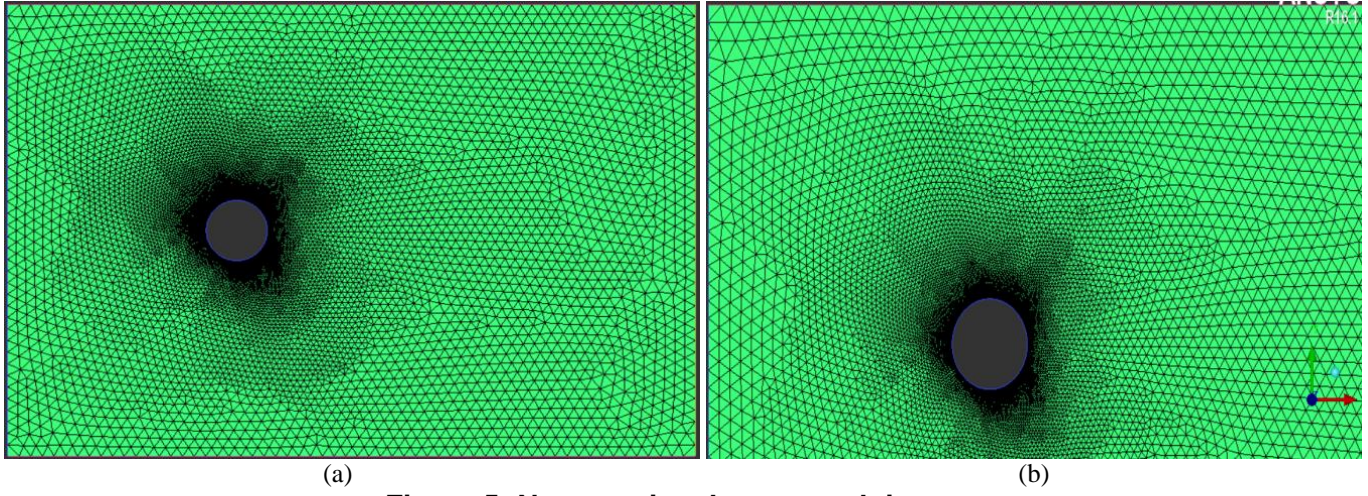


Figure 5: Non-rotational zone mesh images

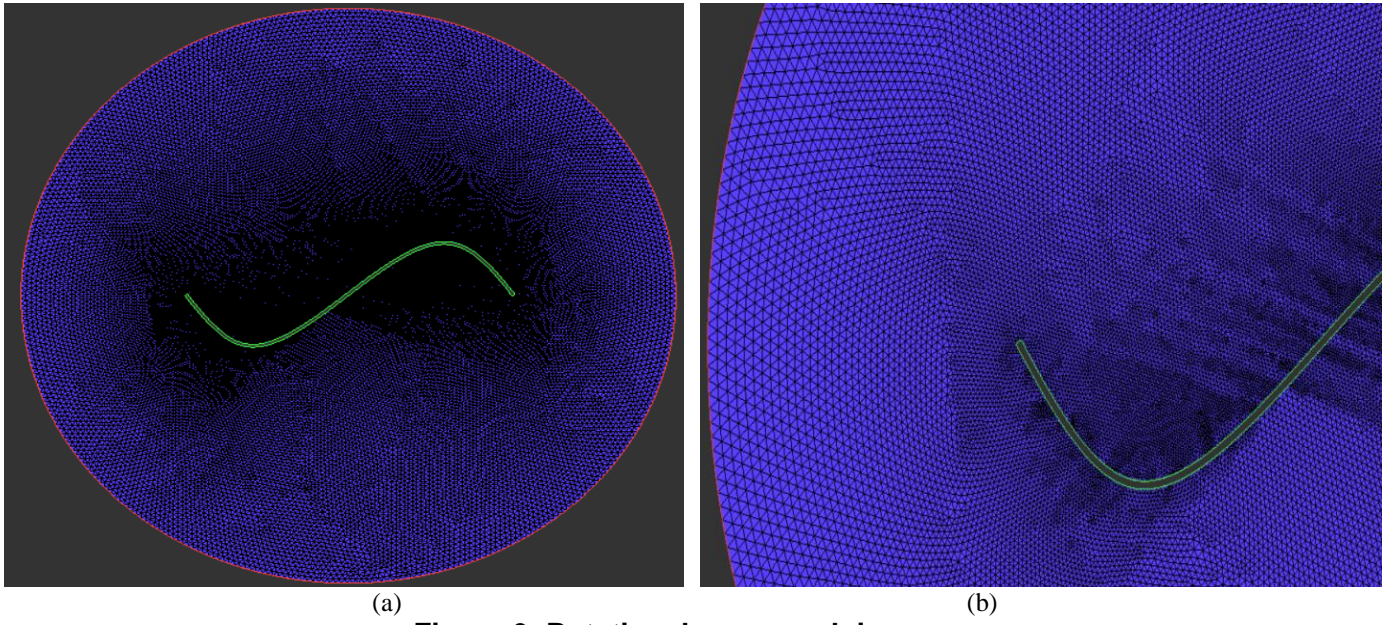


Figure 6: Rotational zone mesh images

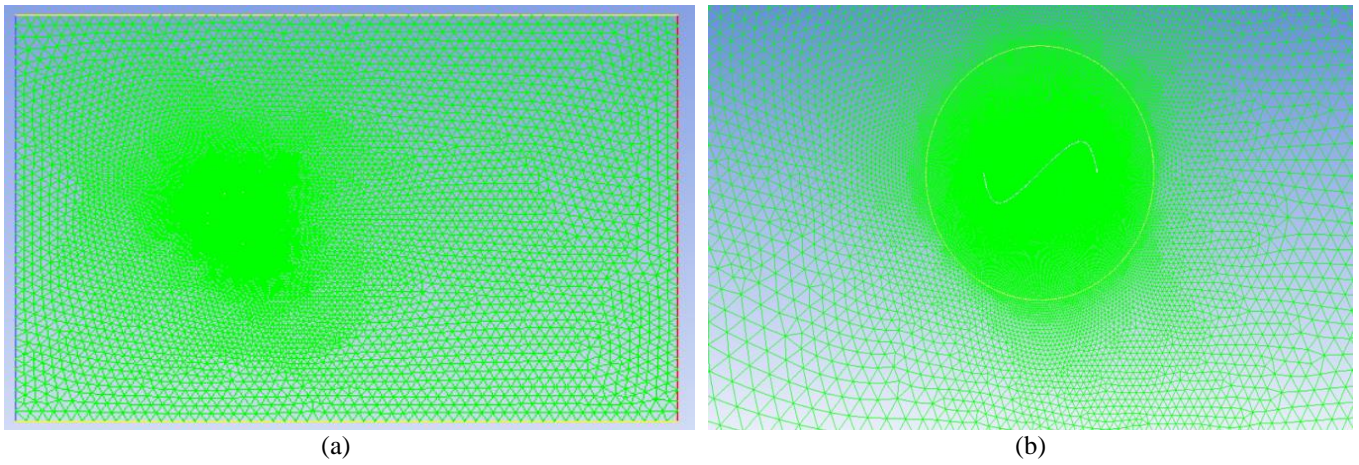


Figure 7: Complete computational domain mesh images

Mesh	No. of elements	C_T	Time (in hours)
1	65000	0.2309	4.25
2	100000	0.2357	6
3	140000	0.2363	8.5

4 RESULTS AND DISCUSSION

In this section, the results of the above performed optimization procedure coupled with *CFD* simulations is carried out for 25 iterations to obtain a new optimum blade profile are discussed and compared to the semicircular profile results. The constant parameters used in the simplex search method are γ , β and ϵ having values 0.5, 2 and 10^{-4} respectively. The computational tasks are carried out in MATLAB version 2014a, ANSYS ICEMCFD 16.1 and ANSYS Fluent 16.1 [14, 15]. The whole process is carried out on the system with 3.7 GHz Intel Xeon processor housing 16 GB RAM. Windows 10 Pro 64 bit is the operating system.

4.1 Optimal Blade Geometry

The optimal solution obtained after completing 25 iterations of the Simplex Search Method is depicted in Table 2 along with the C_T and C_P value for the semi-circular profile

blade. The value of decision variable for the optimal profile is (75.4766, 48.0479). The gradual improvement in the C_T value through the applied procedure is briefly shown in Table 3. It depicts the best C_T values obtained over several iterations along with the corresponding values of the decision variable which forms the blade profile. Figure 8 shows the change in the C_T values with respect to the number of iterations. It can be seen that the solution improves many folds and gets stagnant around 25 iterations. Figure 9 shows the corresponding best blade profiles in each iteration for over 25 iterations. Since the profiles are all symmetric, only half of the profile lying in the first quadrant is shown in this figure. However, Figure 10 shows the newly obtained optimal blade profile.

Profile	C_T	C_P
Semi-circular	0.293	0.23
Optimum	0.328	0.26

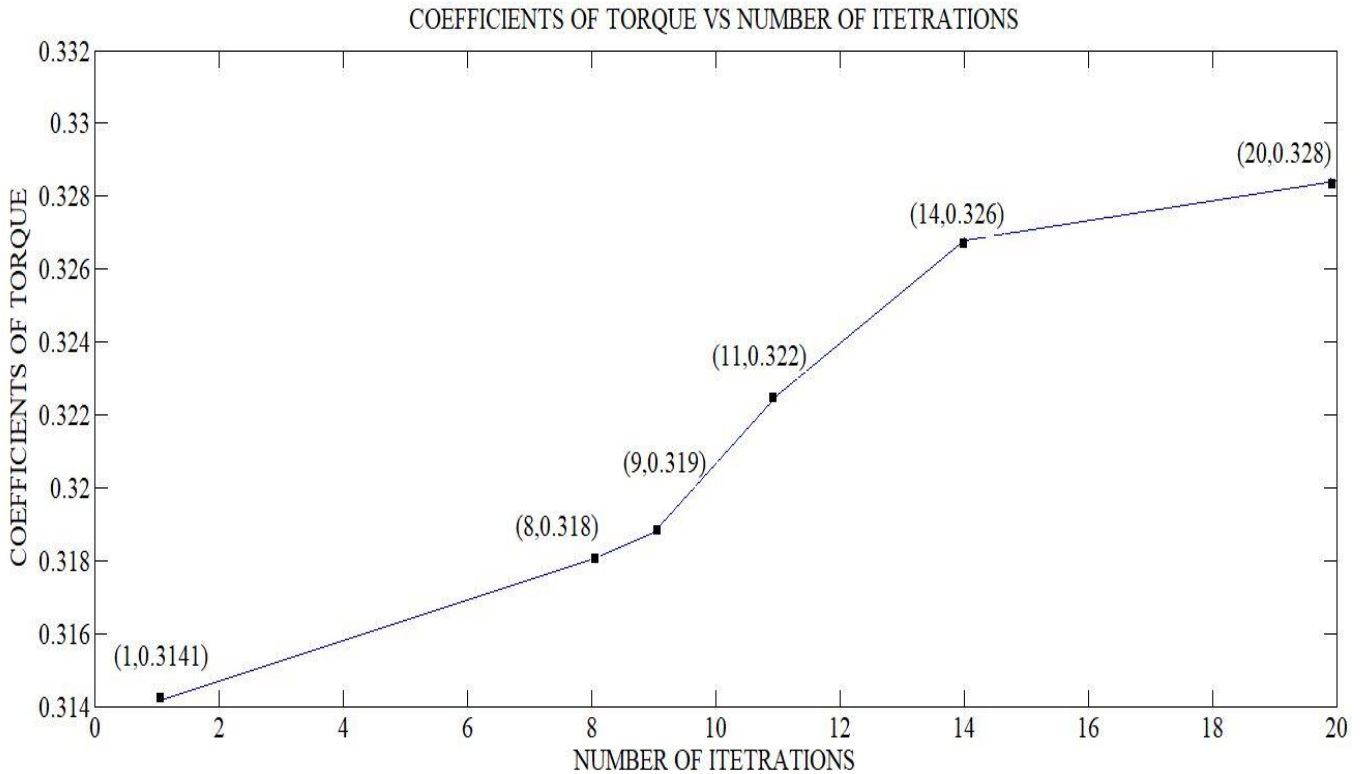
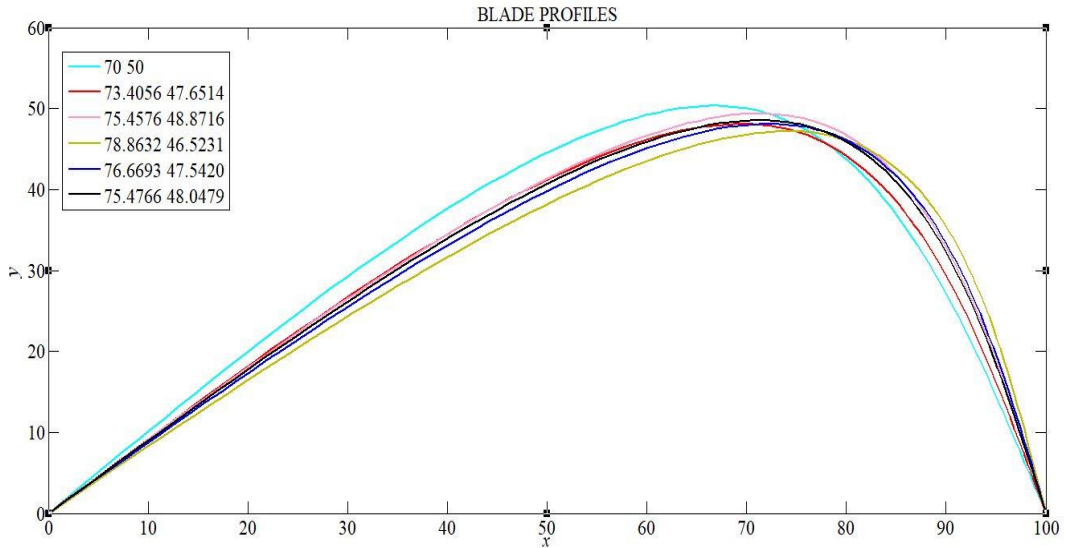
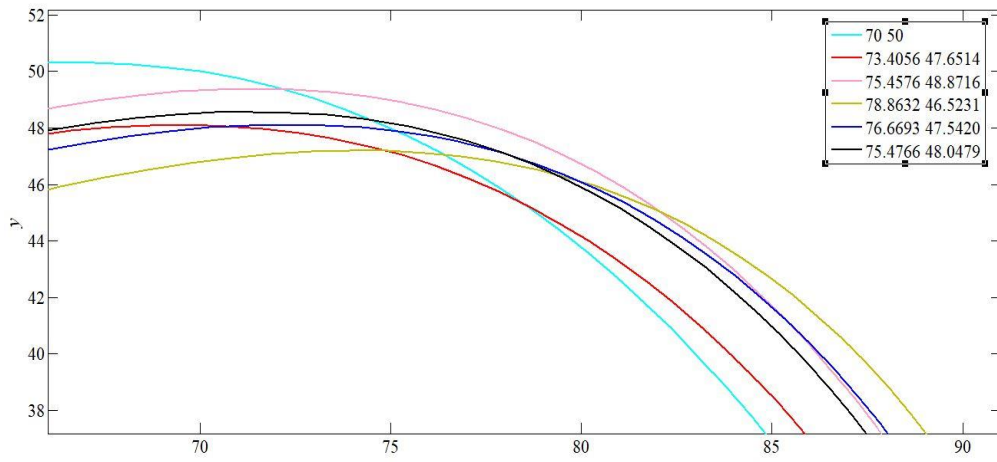


Figure 8: Coefficient of Torque vs. Number of Iterations



(a)



(b)

Figure 9: Corresponding blade profiles of the design variables in Table 3

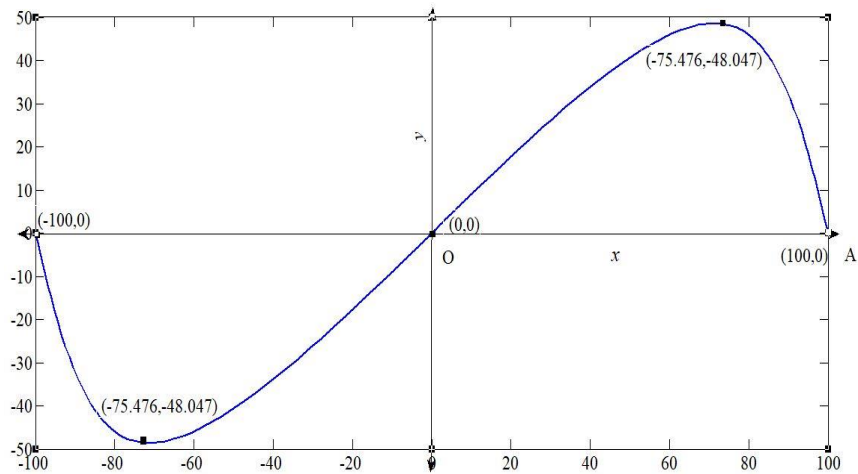


Figure 10: Blade Skeleton of the optimum profile

Sl. No.	Number of Iterations	Colour	Design Variables	C_T
1	1	Light Blue	(70, 50)	0.314
2	8	Red	(73.4056, 47.6514)	0.318
3	9	Pink	(75.4576, 48.8716)	0.319
4	11	Yellow	(78.8632, 46.5231)	0.322
5	14	Blue	(76.6693, 47.542)	0.326
6	20	Black	(75.4766, 48.0479)	0.328

4.2 Effect of TSR

Figure 11 shows the comparison between the C_P values of the new blade profile and the semicircular blade profile over a TSR range of 0.6 to 1 in order to check the feasibility of the new profile for its applications in the urban environment. It is found that the new optimal blade profile performs better than the semi-circular profile in the given TSR range.

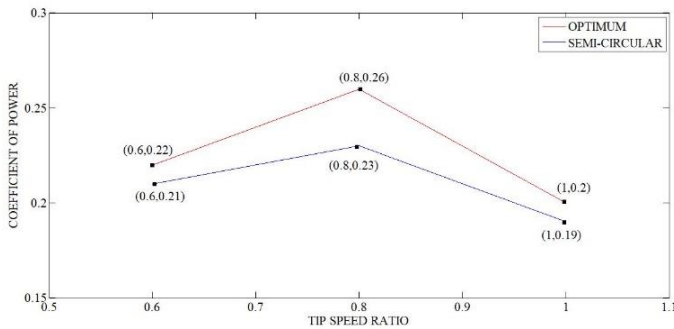
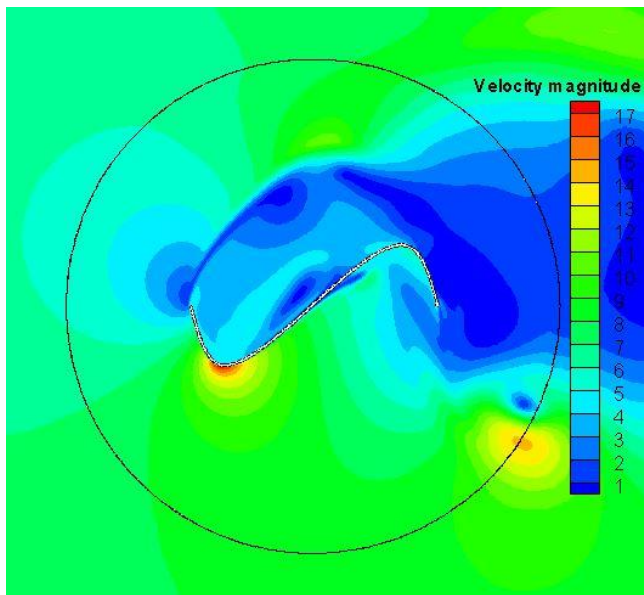


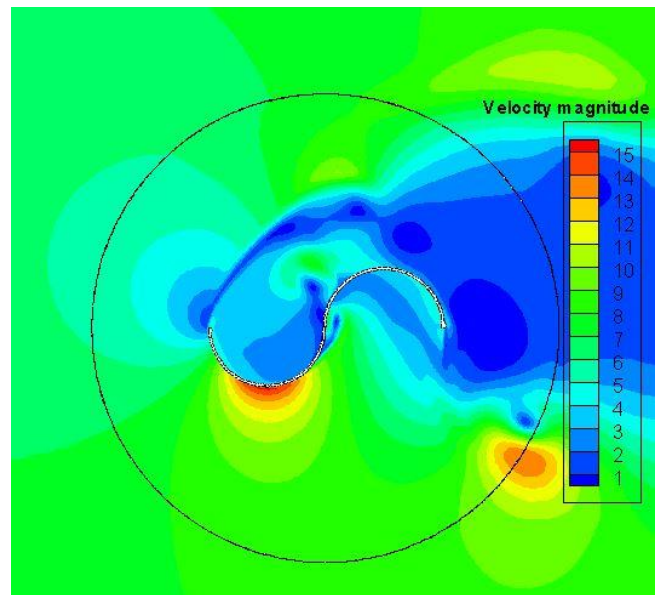
Figure 11: Comparison of C_P for semicircular and optimum blade for different TSR

4.3 Analysis of Velocity Contours

Figure 12 shows the velocity magnitude contours of the optimum and the semi-circular profiles for $TSR = 0.8$. On the concave side of the advancing blade, the velocity magnitude of the optimum profile ranges between 3 to 6 m/s, while for semicircular profile it ranges between 1 to 4 m/s. On the convex side of the advancing blade, the velocity magnitude for the optimum profile ranges between 8 to 17 m/s, while for semicircular profiles it ranges between 7 to 15 m/s but it covers a much larger area of the blade than the new profile. Therefore, the advancing blade of the new profile experiences much lesser negative drag than the semi-circular profile. Now, for the returning blade, the velocity magnitude on the concave side of the new profile is more than that of the semicircular profile and the velocity magnitude on the convex side is again much lesser than that of the semicircular profile. This again ensures that the negative drag on the returning blade is lesser for the new profile as compared to the semicircular profile. Since the Savonius turbine is a drag-based machine, the lesser value of the negative drag helps to obtain a higher C_T value which in turn improves the turbine performance.



(a) Optimum Profile



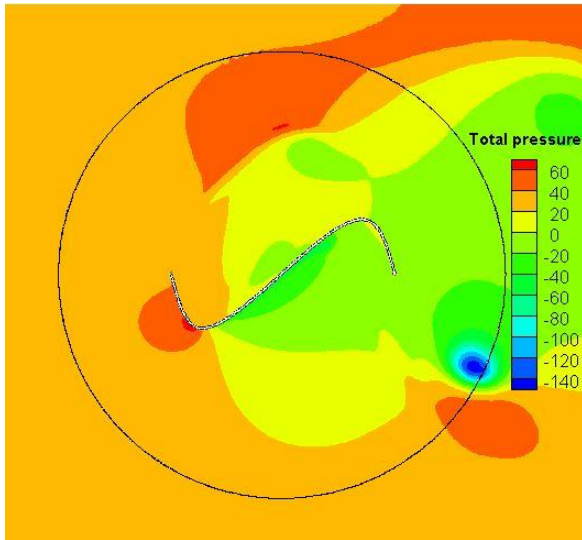
(b) Semicircular Profile

Figure 12: Velocity magnitude (m/s) contours at $TSR = 0.8$

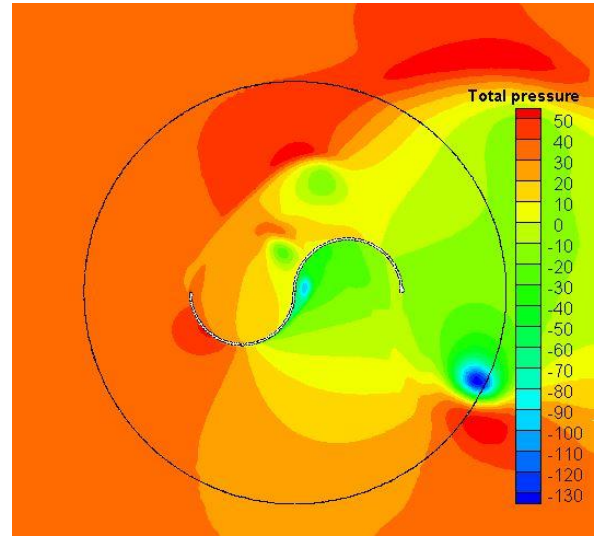
4.4 Analysis of Total Pressure Contours

Figure 13 shows the total pressure contours of the optimum and the semi-circular profiles for $TSR = 0.8$. The total pressure for the new as well as semicircular profiles near the advancing blade ranges between 0 to 40 N/m^2 on the concave side and from -40 to 60 N/m^2 on the convex side. Also for the

returning blade, the pressure on the convex side is greater than the concave side for both the profiles. This is an unfavourable condition. However, this pressure difference is relatively lower in case of optimum profile as compared to the semicircular profile. Thus, the turbine performance is improved.



(a) Optimum Profile



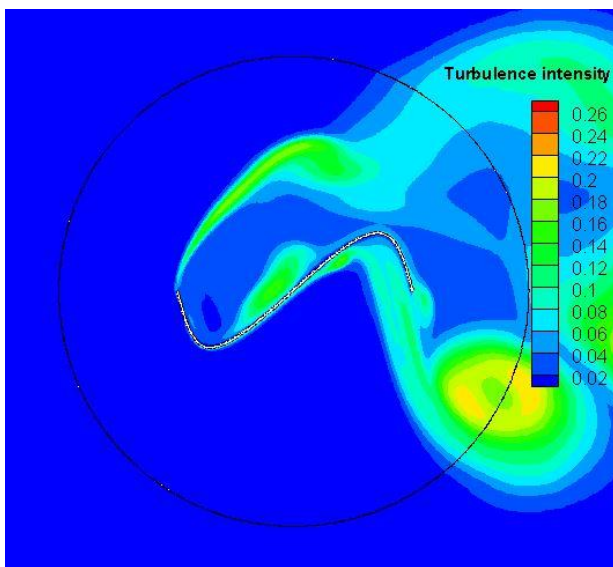
(b) Semicircular Profile

Figure 13: Total Pressure (N/m^2) contours at $TSR = 0.8$

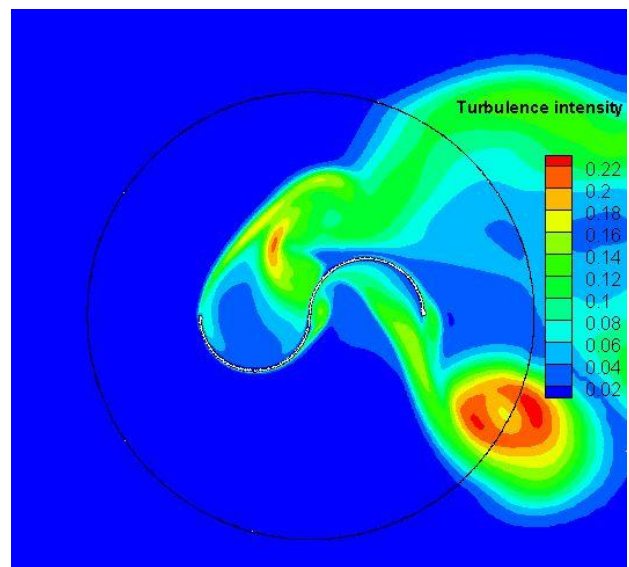
4.5 Analysis of Turbulent Intensity Contours

Figure 14 shows the turbulent intensity contours of the new and the semi-circular profiles for a TSR value of 0.8. The magnitude of turbulence intensity ranges from 0 to 0.16 for the

new profile, while it varies from 0 to 0.22 for the semicircular profile. It can also be seen that in the case of semicircular profile, the turbulence intensity is higher at the downstream which can lead to the formation of vortices and reduces the performance of the turbine.



(a) Optimum Profile



(b) Semicircular Profile

Figure 14: Turbulence intensity (%) contours at $TSR = 0.8$

5 CONCLUSION AND FUTURE SCOPE

The Savonius wind turbines have a lot of potential of harvesting the wind energy in environments where large area of land is not available, owing to its simplistic design, compact size, low cost and several other factors. Still, its relatively lower efficiency has attracted a lot of numerical and experimental studies on the topic and as a result, several new profiles were developed using trial and error approach. In the current investigation, an attempt has been made to optimize the blade shape profile of the Savonius wind turbine by incorporating 2D transient *CFD* simulations in the Simplex Search Method. The generated blade profile is then further compared with the semicircular blade profile over a range of *TSR* to check its feasibility in practical applications. The C_P of the generated and the semicircular profiles is found to be 0.26 and 0.23, respectively. Hence, there is an improvement in the performance of the turbine. It is also noticed that the performance of the generated blade profile is better than the semicircular blade profile for the *TSR* range 0.6 – 1. The velocity magnitude, total pressure and turbulence intensity contours have been plotted and the analysis justifies the improved performance of the generated blade profile.

In the present work, the overlap ratio (*OR*) and separation gap (*SG*) were taken as 0. Therefore, further studies involving the use of optimum *OR* and *SG* in the geometry, can help improve the performance of the obtained blade.

REFERENCES

- [1] V. J. Modi and M. S. U. K. Fernando, "On the Performance of the Savonius Wind Turbine," *J. Sol. Energy Eng.*, vol. 111, no. 1, p. 71, 1989.
- [2] N. Fujisawa, "On the Torque mechanism of Savonius Rotors," *J. Wind Eng. Ind. Aerodyn.*, vol. 40, no. 3, pp. 277–292, 1992.
- [3] R. Gupta, A. Biswas, and K. K. Sharma, "Comparative Study of a Three-bucket Savonius Rotor with a Combined Three-bucket Savonius-three-bladed Darrieus Rotor," *Renew. Energy*, vol. 33, no. 9, pp. 1974–1981, 2008.
- [4] U. K. Saha, S. Thotla, and D. Maity, "Optimum Design Configuration of Savonius Rotor Through Wind Tunnel Experiments," *J. Wind Eng. Ind. Aerodyn.*, vol. 96, no. 8–9, pp. 1359–1375, 2008.
- [5] N. H. Mahmoud, A. A. El-Haroun, E. Wahba, and M. H. Nasef, "An Experimental Study on Improvement of Savonius Rotor Performance," *Alexandria Eng. J.*, vol. 51, no. 1, pp. 19–25, 2012.
- [6] K. S. Jeon, J. I. Jeong, J. K. Pan, and K. W. Ryu, "Effects of End Plates with Various Shapes and Sizes on Helical Savonius Wind Turbines," *Renew. Energy*, vol. 79, no. 1, pp. 167–176, 2015.
- [7] J. V. Akwa, G. Alves Da Silva Júnior, and A. P. Petry, "Discussion on the Verification of the Overlap Ratio Influence on Performance Coefficients of a Savonius Wind Rotor Using Computational Fluid Dynamics," *Renew. Energy*, vol. 38, no. 1, pp. 141–149, 2012.
- [8] S. Roy and U. K. Saha, "Computational Study to Assess the Influence of Overlap Ratio on Static Torque Characteristics of a Vertical Axis Wind Turbine," *Procedia Eng.*, vol. 51, pp. 694–702, 2013.
- [9] N. Alom and U. K. Saha, "Performance Evaluation of Vent-augmented Elliptical-bladed Savonius Rotors by Numerical Simulation and Wind Tunnel Experiments," *Energy*, vol. 152, pp. 277–290, 2018.
- [10] S. Roy, R. Das, and U. K. Saha, "An Inverse Method for Optimization of Geometric Parameters of a Savonius-style Wind Turbine," *Energy Convers. Manag.*, vol. 155, pp. 116–127, 2018.
- [11] C. M. Chan, H. L. Bai, and D. Q. He, "Blade Shape Optimization of the Savonius Wind Turbine Using a Genetic Algorithm," *Appl. Energy*, vol. 213, no. August 2017, pp. 148–157, 2018.
- [12] Q. Zhou, Z. Xu, S. Cheng, Y. Huang, and J. Xiao, "Innovative Savonius Rotors Evolved by Genetic Algorithm Based on 2D-DCT Encoding," *Soft Comput.*, no. 2016, pp. 1–10, 2018.
- [13] A. Ravindran, K. M. Ragsdell, and G. V. Reklaitis, "Engineering Optimization: Methods and Applications," Wiley Publications, 2nd edition, 2006.
- [14] ANSYS Inc, 2009. ANSYS Fluent Theory Guide 12.0.
- [15] ANSYS Inc, 2015. ANSYS Fluent Theory Guide 12.0